

# Testing nuclear forces by polarization transfer coefficients in $d(\vec{p}, \vec{p})d$ and $d(\vec{p}, \vec{d})p$ reactions at $E_p^{lab} = 22.7$ MeV

H. Witała<sup>1</sup>, J. Golak<sup>1</sup>, R. Skibiński<sup>1</sup>, W. Glöckle<sup>2</sup>, A. Nogga<sup>3</sup>, E. Epelbaum<sup>4</sup>, H. Kamada<sup>5</sup>,  
A. Kievsky<sup>6</sup>, M. Viviani<sup>6</sup>

<sup>1</sup>*M. Smoluchowski Institute of Physics, Jagiellonian University, PL-30059 Kraków, Poland*

<sup>2</sup>*Institut für Theoretische Physik II, Ruhr-Universität Bochum, D-44780 Bochum, Germany*

<sup>3</sup>*Institut für Kernphysik, Forschungszentrum Jülich, D-52425 Jülich, Germany*

<sup>4</sup>*Jefferson Laboratory, Theory Division, Newport News, VA 23606, USA*

<sup>5</sup>*Department of Physics, Faculty of Engineering, Kyushu Institute of Technology, 1-1 Sensuicho,  
Tobata, Kitakyushu 804-8550, Japan*

<sup>6</sup>*Istituto Nazionale di Fisica Nucleare, Via Buonarroti 2, I-56100 Pisa, Italy*

(September 29, 2018)

## Abstract

The proton to proton polarization transfer coefficients  $K_x^{x'}$ ,  $K_y^{y'}$ ,  $K_z^{x'}$  and the proton to deuteron polarization transfer coefficients  $K_x^{x'}$ ,  $K_y^{y'}$ ,  $K_z^{x'}$ ,  $K_x^{y'z'}$ ,  $K_y^{z'z'}$ ,  $K_z^{y'z'}$ ,  $K_y^{x'z'}$  and  $K_y^{x'x'-y'y'}$  have been measured in  $d(\vec{p}, \vec{p})d$  and  $d(\vec{p}, \vec{d})p$  reactions at  $E_p^{lab} = 22.7$  MeV, respectively. The data have been compared to predictions of modern nuclear forces obtained by solving the three-nucleon Faddeev equations in momentum space. Realistic (semi) phenomenological nucleon-nucleon potentials combined with model three-nucleon forces and modern chiral nuclear forces have been used. The AV18, CD Bonn, Nijm I and II nucleon-nucleon interactions have been applied alone or combined with the Tucson-Melbourne 99 three-nucleon force, adjusted separately for each potential to reproduce the triton binding energy. For the AV18 potential also the Urbana IX three-nucleon force have been used. In addition chiral NN potentials in the next-to-leading-order and chiral two- and three-nucleon forces in the next-to-next-to-leading-order have been applied. Only when three-nucleon forces are included a satisfactory description of all data results. For the chiral approach the restriction to the forces in the next-to-leading order is insufficient. Only when going over to the next-to-next-to-leading order one gets a satisfactory description of the data, similar to the one obtained with the (semi) phenomenological forces.

21.45.+v, 24.70.+s, 25.10.+s, 25.40.Lw

## I. INTRODUCTION

A rich set of observables provided by three-nucleon (3N) reactions can be used to test modern nuclear forces. Presently there are two theoretical approaches to construct them. In the traditional approach the nucleon-nucleon (NN) potentials are derived in the framework of the meson-exchange picture alone or mixed with phenomenological assumptions. By adjusting parameters so called realistic, high precision interactions such as the phenomenological AV18 [1] potential and the meson-theoretical CD Bonn [2] together with Nijm I and II [3] potentials are obtained. They provide a very good description of NN data below about 350 MeV nucleon laboratory energy. All these potentials have in common that they fit the large set of NN data with  $\chi^2$  per datum close to one, indicating essentially phase equivalence.

In a more modern framework of chiral effective field theory, nuclear forces are linked to the underlying strong interaction between quarks and gluons. They are derived from the most general effective Lagrangian for pions and nucleons, which is consistent with the spontaneously broken approximate chiral symmetry of QCD, using chiral perturbation theory ( $\chi$ PT) [4]. The  $\chi$ PT approach gives a deeper understanding of nuclear forces than the traditional approach and allows to construct three- and more-nucleon forces consistent with the NN interactions [5–7]. In practice, various contributions to the nuclear force in the  $\chi$ PT framework are organized in terms of the expansion in  $Q/\Lambda$ , where  $Q$  is the soft scale corresponding to the nucleon external momenta and the pion mass and  $\Lambda$  is the hard scale associated with the chiral symmetry breaking scale or an ultraviolet cut-off. At present, the two-nucleon system has been studied up to next-to-next-to-next-to-leading order (NNNLO) in the chiral expansion [7,8]. At this order, the two-nucleon force receives the contributions from one-pion exchange, two-pion exchange at the two-loop level as well as three-pion exchange, which turn out to be numerically irrelevant. In addition, one has to take into account all possible short-range contact interactions with up to four derivatives and the appropriate isospin-breaking effects. In the three- and more-nucleon sectors, the calculations have so far only been performed up to next-to-next-to-leading order (NNLO) [7]. In this work, we will show the results corresponding to the latest version of the chiral NN forces introduced in references [9,8] and based on the spectral function regularization scheme [10].

Recent studies of few-nucleon bound states and of 3N reactions provided numerous indications that three-nucleon forces (3NFs) form an important component of the potential energy of three interacting nucleons [11–16]. In the traditional approach they are accounted for by adding model 3NFs, such as e.g. the  $2\pi$ -exchange Tucson-Melbourne (TM) [17] or Urbana IX [18] interactions, with parameters adjusted to reproduce the experimental triton binding energy. Such a simple treatment allows to cure some of the discrepancies between data and theory [19–25]. In the approach based on  $\chi$ PT nonvanishing 3NFs appear in the next-to-next-to-leading order (NNLO) of the chiral expansion. In addition to the  $2\pi$ -exchange term two other topologies appear. One of them corresponds to a contact interaction of three nucleons and the second to a contact interaction of two nucleons exchanging in addition one pion with the third nucleon. The two free parameters of these two terms are adjusted by fitting two independent 3N observables (e.g. the triton binding and the nd doublet scattering length). The quality of the description of the 3N observables is then

similar in both approaches [26]. The study of the details of the 3NF's is a lively topic of present day few-nucleon system studies.

In the present paper we would like to analyze the proton to proton and the proton to deuteron spin transfer coefficients measured in  $d(\vec{p}, \vec{p})d$  and  $d(\vec{p}, \vec{d})p$  reactions, respectively, at  $E_p^{lab} = 22.7$  MeV [27–29]. The existing data for polarization transfer coefficients in elastic nucleon-deuteron (Nd) scattering are restricted to few experiments in the pd system ( $E_p^{lab} = 10$  MeV [30],  $E_p^{lab} = 19$  MeV [31],  $E_p^{lab} = 250$  MeV [23],  $E_d^{lab} = 270$  MeV [32]) and to one measurement in the nd system ( $E_p^{lab} = 19$  MeV [33]). After a short description of the theoretical calculations in Section II in section III we show the data and compare them to different theoretical predictions. The summary and conclusions follow in Section IV.

## II. CALCULATIONS

In this work we will employ two different methods to solve the nucleon-deuteron scattering problem. Our first scheme is based on Faddeev equations. The nucleon-deuteron elastic scattering with neutron and protons interacting through a NN potential  $V$  and through a 3NF  $V_4$  is described in terms of a breakup operator  $T$  satisfying the Faddeev-type integral equation [34,15,35]

$$T = tP + (1 + tG_0)V_4^{(1)}(1 + P) + tPG_0T + (1 + tG_0)V_4^{(1)}(1 + P)G_0T. \quad (1)$$

The two-nucleon (2N) t-matrix  $t$  results from the interaction  $V$  through the Lippmann-Schwinger equation. The permutation operator  $P = P_{12}P_{23} + P_{13}P_{23}$  is given in terms of the transposition  $P_{ij}$  which interchanges nucleons  $i$  and  $j$  and  $G_0$  is the free 3N propagator. Finally the operator  $V_4^{(1)}$  appearing in Eq.(1) is part of the full 3NF  $V_4 = V_4^{(1)} + V_4^{(2)} + V_4^{(3)}$  and is symmetric under exchange of nucleons 2 and 3. For instance, in the case of the  $\pi - \pi$  exchange 3NF such a decomposition corresponds to the three possible choices of the nucleon which undergoes off-shell  $\pi - N$  scattering. It is understood that the operator  $T$  acts on the incoming state  $|\phi\rangle = |\vec{q}_0\rangle |\phi_d\rangle$  which describes the free nucleon-deuteron motion with relative momentum  $\vec{q}_0$  and the deuteron wave function  $|\phi_d\rangle$ . The physical picture underlying Eq.(1) is revealed after iteration which leads to a multiple scattering series for  $T$ .

The elastic Nd scattering transition operator  $U$  is given in terms of  $T$  by [34,15,35]

$$U = PG_0^{-1} + PT + V_4^{(1)}(1 + P) + V_4^{(1)}(1 + P)G_0T. \quad (2)$$

We solve Eq.(1) in momentum space using a partial wave decomposition for each total angular momentum  $J$  and parity of the 3N system. To achieve converged results a sufficiently high number of partial waves have been used. Calculations with and without 3NF were performed including all 3N partial wave states with total two-body angular momenta up to  $j = 5$ . In the case when the 3NF is switched-off Eq.(1) is solved for  $J$  up to  $25/2$ . When the shorter ranged 3NF is also active it is sufficient to go up to  $J \leq 13/2$  only. In all calculations we neglect the total isospin  $T = 3/2$  contribution in the  $^1S_0$  state and use in this state a np form of the NN interaction. Such a restriction to the np force for the  $^1S_0$  state does not have a significant effect on the polarization transfer coefficients.

The second scheme is based on the Kohn Variational principle, the  $S$ -matrix elements corresponding to a 3N scattering state with total angular momentum  $J$  can be obtained as the stationary point of the functional

$$[^J S_{LL'}^{SS'}] = {}^J S_{LL'}^{SS'} + i \langle \Psi_{LSJ}^- | H - E | \Psi_{L'S'J}^+ \rangle. \quad (3)$$

The wave function  $\Psi_{LSJ}^+$  describes a 3N scattering state in which asymptotically an ingoing nucleon is approaching the deuteron in a relative angular momentum  $L$  and total spin  $S$ . The parity of the state is given by  $(-1)^L$ . The wave function is expanded, using a partial wave decomposition, in terms of the pair correlated hyperspherical harmonic (PHH) basis as described in Ref. [25]. As in the Faddeev scheme, states up to  $J = 25/2$  have been considered.

In our Faddeev calculations the Coulomb interaction between two protons is totally neglected. A measurement of the neutron to neutron polarization transfer coefficients  $K_y^{y'}$  in neutron-deuteron (nd) elastic scattering [33] and their comparison to the corresponding pd data [31] shows that effects caused by the Coulomb force for this coefficient are non-negligible. These effects have been studied on a few polarization transfer coefficients [36] as well as in other polarization observables [25] using the Kohn variational principle in conjunction with the PHH basis. In these calculations the Coulomb force between the two protons has been considered without approximations and the results confirm sizable Coulomb-force effects in the energy range considered here. Therefore to remove possible Coulomb-force effects for the studied polarization transfer coefficients we proceed in the following manner. Using the PHH expansion we evaluate the studied polarization transfer coefficients without and with Coulomb force and employ the AV18 NN interaction. This is displayed in Figs. 1-3. In this manner we read off the shifts caused by the pp Coulomb force. Then we generate “nd” data by applying those shifts to our pd data. For the studied polarization transfers the Coulomb force effects are restricted mostly to forward angles and to the region around  $\theta_{cm} \approx 120^\circ$ . For the proton to proton spin transfer coefficient  $K_x^{x'}$  they are of minor importance whereas for  $K_y^{y'}$  and  $K_z^{z'}$  the Coulomb force effects change significantly the magnitude of these coefficients around  $\theta_{cm} \approx 120^\circ$  (see Fig. 1). For the proton to vector-deuteron spin transfers Coulomb force effects are rather small with exception of very forward angles, where they decrease significantly the magnitude (see Fig. 2). For  $K_z^{z'}$  also some effects are seen around  $\theta_{cm} \approx 120^\circ$ . In case of the proton to tensor-deuteron transfers shown in Fig. 3 only  $K_x^{y'z'}$  (in the steep slope),  $K_y^{x'z'}$  and  $K_z^{y'z'}$  exhibit large Coulomb force effects in the region of cm angles around  $\theta_{cm} \approx 120^\circ$ . In the following figures we include both, the pd and “nd” data.

### III. RESULTS

In Figs. 4-6 we show our data and compare them to theoretical predictions based on (semi)phenomenological NN potentials alone or combined with the TM99 [37] or Urbana IX [18] 3NFs, which have been obtained in the Faddeev approach, where we are able to employ also non-local interactions. The corresponding comparison for chiral forces is presented in Figs. 7-9. Comparison with experiment always means the Coulomb corrected “nd” data.

For the traditional approach based on high quality (semi)phenomenological interactions, we have taken the NN potentials AV18, CDBonn, Nijm I and II and combined each of them

with the  $2\pi$ -exchange TM99 3NF, adjusting the cut-off parameter of TM99 individually to get the experimental triton binding energy. The resulting cut-offs for these potentials are respectively 5.215, 4.856, 5.120 and 5.072 (in units of the pion mass  $m_\pi$ ). From the predictions of these potentials alone or combined with the TM99 3NF two bands, light and dark, respectively, were formed and shown in Figs. 4-6.

For the proton to proton spin transfer coefficients (see Fig. 4) the effects of the Coulomb interaction are located in the region of c.m. angles around  $\theta_{cm} \approx 120^\circ$ . In that region the differential cross section has its minimum. They are significant only for  $K_y^{y'}$  and  $K_z^{x'}$  and are practically negligible for  $K_x^{x'}$ . The realistic potentials alone provide a good description only of  $K_x^{x'}$  and fail to reproduce the data for  $K_y^{y'}$  and  $K_z^{x'}$ , especially around  $\theta_{cm} \approx 120^\circ$ . Including the TM99 3NF, and in case of AV18 also Urbana IX, changes only slightly the predictions for  $K_x^{x'}$ . For  $K_y^{y'}$  and  $K_z^{x'}$  the effects of these 3NFs are significant in the region of c.m. angles around  $\theta_{cm} \approx 120^\circ$  and their inclusion leads to a good description of the data.

For the corresponding proton to deuteron spin transfer coefficients ( $K_x^{x'}$ ,  $K_y^{y'}$  and  $K_z^{x'}$  - see Fig. 5) effects of the Coulomb force are practically negligible at angles where data exist and they are seen only for  $K_z^{x'}$ . For these observables also effects of the TM99 and Urbana IX 3NFs are small and the realistic NN potentials alone or combined with these 3NFs provide quite good description of the data.

For the proton to tensor-deuteron spin transfer coefficients the Coulomb forces are significant for  $K_x^{y'z'}$ ,  $K_y^{x'z'}$ , and  $K_z^{y'z'}$  (see Fig. 6). In case of  $K_y^{z'z'}$  and  $K_y^{x'x'-y'y'}$  (see Fig. 6) they are negligible at angles where data exist. For these two coefficients also the effects of the TM99 and Urbana IX 3NFs are small and the NN potentials alone provide a good description of data. This is similar for  $K_x^{y'z'}$ . For  $K_y^{x'z'}$  and  $K_z^{y'z'}$  the effects of these 3NFs are nonnegligible, especially in the region of angles around  $\theta_{cm} \approx 120^\circ$ . While for  $K_y^{x'z'}$  the inclusion of the TM99 or Urbana IX 3NFs improves the description of the data, in case of  $K_z^{y'z'}$  it shifts the theory away from the data points.

Based on the chiral interactions we show in Figs. 7-9 two bands of predictions based on forces derived in NLO and NNLO. Each band is based on five predictions obtained with different cut-off combinations: (450,500), (600,500), (550,600), (450,700), and (600,700) (see [7] for more details). The results for the chiral NN potentials in NLO are shown by the light band. In NNLO the first time nonzero contributions from chiral three-nucleon interactions arise and the predictions based on the full chiral Hamiltonian in NNLO are shown by the dark band.

It is clearly seen that the restriction to NLO only is quite insufficient even at low energy of our experiment. The predictions based on the chiral NN potential obtained in this low order are far away from the data. At NNLO one could show the NN force predictions alone. We refrain from doing that since this is ambiguous. As is well known unitarily transformed 2N forces, which do not affect two nucleon observables, lead to different results in the 3N system [38]. It is only the complete 3N Hamiltonian which provides unambiguous results for the 3N observables. Since the chiral approach systematically improves the nuclear force description with increasing order and provides strong internal links between 2N forces and forces beyond, we deviate here from the usual presentation exhibiting 3N force effects separately. This was done above in the standard approach since anyhow there is no internal consistency between NN and 3N forces. Now a view on Figs. 7-9 shows that the full NNLO predictions lead to a quite good description as the traditional approach including 3N forces. The exception are

$K_y^{y'}$  for the proton to proton transfer, where the chiral approach differs from the data and  $K_z^{y'z'}$  for the proton to deuteron transfer, where it leads to an agreement with the data. In the standard approach it is opposite.

It will be of great interest to see the outcome for NNNLO, where the NN forces have already been worked out [8]. At that order there contribute a whole host of parameter free 3NFs including first relativistic effects.

#### IV. SUMMARY AND CONCLUSIONS

We presented new data for spin transfer coefficients in elastic pd scattering, both for the proton to proton and for the proton to deuteron transfers. They have been measured using a polarized proton beam with energy  $E_p^{lab} = 22.7$  MeV. The data have been corrected for Coulomb force effects using our theoretical framework of a hyperspherical expansion. This leads to “nd” data to which we compare our theory. In some cases the Coulomb force effects are quite significant, especially at  $\theta_{cm} \approx 120^\circ$ , where the differential cross section has its minimum. The theoretical predictions are obtained by solving the 3N Faddeev equations with two different dynamical inputs. One is the standard approach of so called high precision NN forces supplemented by the TM99 and Urbana IX 3NF. The other is an effective field theory approach constrained by chiral symmetry. In the first case where the forces have mostly phenomenological character we show NN force prediction separately in addition to the results obtained by adding the 3NFs. The inclusion of 3NFs clearly improves the description and the comparison with the data is quite successful. In case of the approach based on the chiral nuclear forces NLO is quite insufficient, but at NNLO the combined dynamics of NN and 3N forces does essentially equally well as the standard approach. Exceptions are the spin transfer coefficients  $K_y^{y'}$  from proton to proton and  $K_z^{y'z'}$  from proton to deuteron. The first is well described in the standard approach but not the second one. Just the opposite is true in the chiral approach.

#### ACKNOWLEDGMENTS

This work has been supported by the Polish Committee for Scientific Research under Grant no. 2P03B00825 and by the U.S. Department of Energy Contract No. DE-AC05-84ER40150 under which the Southeastern Universities Research Association (SURA) operates the Thomas Jefferson Accelerator Facility. The numerical calculations have been performed on the IBM Regatta p690+ of the NIC in Jülich, Germany.

## REFERENCES

- [1] R.B. Wiringa, V.G.J. Stoks, R. Schiavilla, Phys. Rev. C**51**, 38 (1995).
- [2] R. Machleidt, F. Sammarruca, and Y. Song, Phys. Rev. C**53**, R1483 (1996).
- [3] V.G.J. Stoks, R.A.M. Klomp, C.P.F. Terheggen, J.J. de Swart, Phys. Rev. C**49**, 2950 (1994).
- [4] S. Weinberg, Nucl. Phys. B **363**, 3 (1991).
- [5] U. van Kolck, Phys. Rev. C **49**, 2932 (1994).
- [6] E. Epelbaum, W. Glöckle, U.-G. Meißner, Nucl. Phys. A **637**, 107 (1998).
- [7] D.R. Entem, R. Machleidt, Phys. Rev. C **68**, 041001 (2003).
- [8] E. Epelbaum, W. Glöckle, Ulf-G. Meißner, Nucl. Phys. A **747**, 362 (2005).
- [9] E. Epelbaum, W. Glöckle, U.-G. Meißner, Eur. Phys. J. A **19**, 401 (2004).
- [10] E. Epelbaum, W. Glöckle, U.-G. Meißner, Eur. Phys. J. A **19**, 125 (2004).
- [11] J.L. Friar et al., Phys. Lett. B**311**, 4 (1993).
- [12] A. Nogga, D. Hüber, H. Kamada, and W. Glöckle, Phys. Lett. B**409**, 19 (1997).
- [13] S.C. Pieper, V.R. Pandharipande, R.B. Wiringa, and J. Carlson, Phys. Rev. C**64**, 014001 (2001).
- [14] H. Witała, W. Glöckle, D. Hüber, J. Golak, and H. Kamada, Phys. Rev. Lett. **81**, 1183 (1998).
- [15] W. Glöckle, H. Witała, D. Hüber, H. Kamada, J. Golak, Phys. Rep. **274**, 107 (1996).
- [16] A. Nogga et al., Phys. Rev. C**67**, 034004 (2003)
- [17] S.A. Coon et al., Nucl. Phys. A**317**, 242 (1979); S.A. Coon and W. Glöckle, Phys. Rev. C**23**, 1790 (1981).
- [18] B.S. Pudliner et al., Phys. Rev. C**56**, 1720 (1997).
- [19] K. Sekiguchi et al., Phys. Rev. C**65**, 034003 (2002).
- [20] H. Witała et al., Phys. Rev. C**63**, 024007 (2001).
- [21] W.P. Afnalterer et al., Phys. Rev. Lett. **81**, 57 (1998).
- [22] H. Witała et al., Phys. Rev. C**59**, 3035 (1999).
- [23] K. Hatanaka et al., Phys. Rev. C**66**, 044002 (2002).
- [24] R.V. Cadman et al., Phys. Rev. Lett. **86**, 967 (2001).
- [25] A. Kievsky, M. Viviani and S. Rosati, Phys. Rev. C **64**, 024002 (2001)
- [26] E. Epelbaum et al., Phys. Rev. C **66**, 064001 (2002).
- [27] A. Glombik et al., AIP Conference Proceedings 334 on Few Body Problems in Physics, Williamsburg 1994, ed. F. Gross, (AIP Press, New York, 1995) p.486.
- [28] W. Kretschmer, private communication.
- [29] W. Kretschmer et al., AIP Conference Proc. 339 (1995) 335 (Polarization Phenomena in Nuclear Physics, Bloomington, 1994).
- [30] F. Sperisen et al., Nucl. Phys. C**422**, 81 (1984).
- [31] L. Sydow et al., Few-Body Systems **25**, 133 (1998).
- [32] K. Sekiguchi et al., Phys. Rev. C**70**, 014001 (2004).
- [33] P. Hempel et al., Phys. Rev. C**57**, 837 (1998).
- [34] H. Witała, T. Cornelius and W. Glöckle, Few-Body Syst. **3**, 123 (1988).
- [35] D. Hüber, H. Kamada, H. Witała, and W. Glöckle, Acta Phys. Pol. B**28**, 1677 (1997).
- [36] A. Kievsky, S. Rosati and M. Viviani, Phys. Rev. C **64**, 041001(R)
- [37] S.A. Coon and H.K. Han, Few-Body Syst. **30**, 131 (2001).
- [38] W.N. Polyzou, W. Glöckle, Few-Body Syst. **9**, 97 (1990).

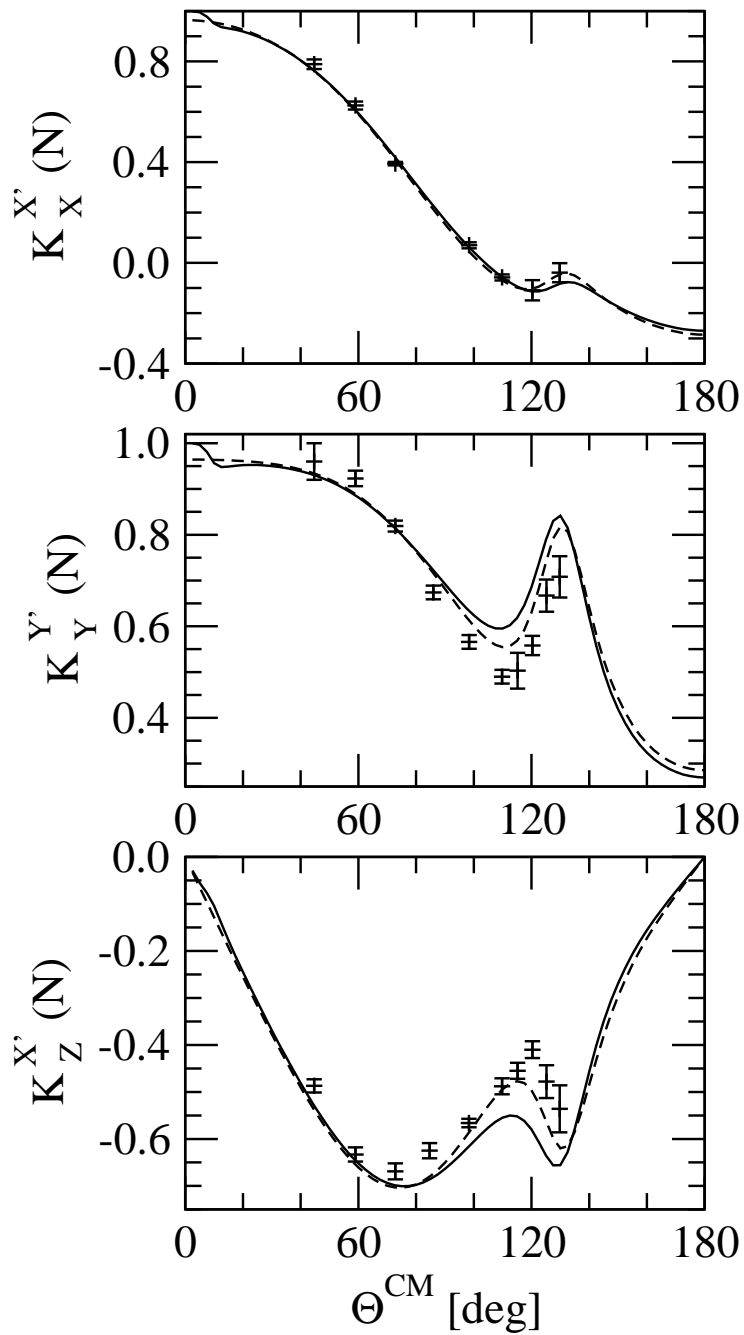


FIG. 1. The nucleon to nucleon spin transfer coefficients in Nd elastic scattering at  $E_{lab}^N = 22.7$  MeV. The crosses are the pd data from [27–29]. The dashed line is the result of the hyperspherical harmonic expansion method with AV18 potential. The solid line is the corresponding result when the pp Coulomb force is included.

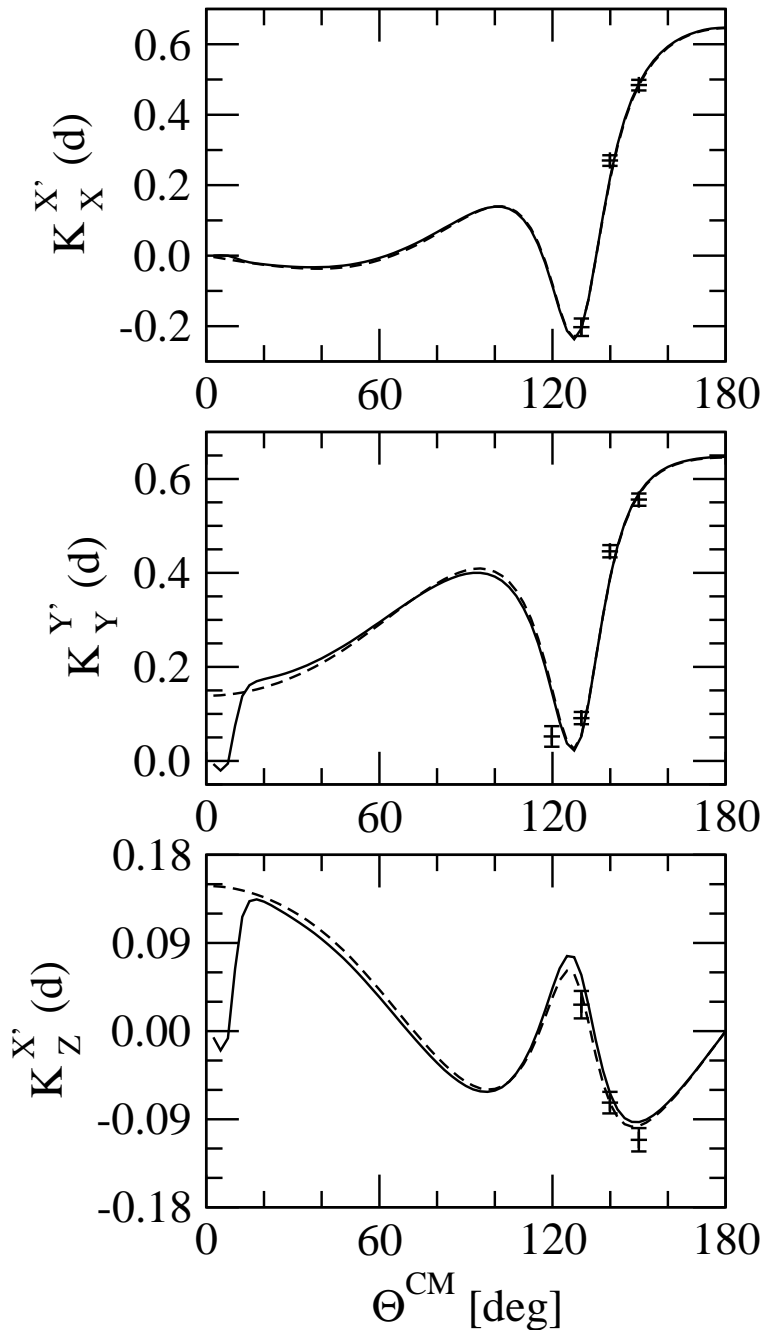


FIG. 2. The nucleon to deuteron spin transfer coefficients in Nd elastic scattering at  $E_{lab}^N = 22.7$  MeV. The description of symbols and lines is the same as in Fig.1.

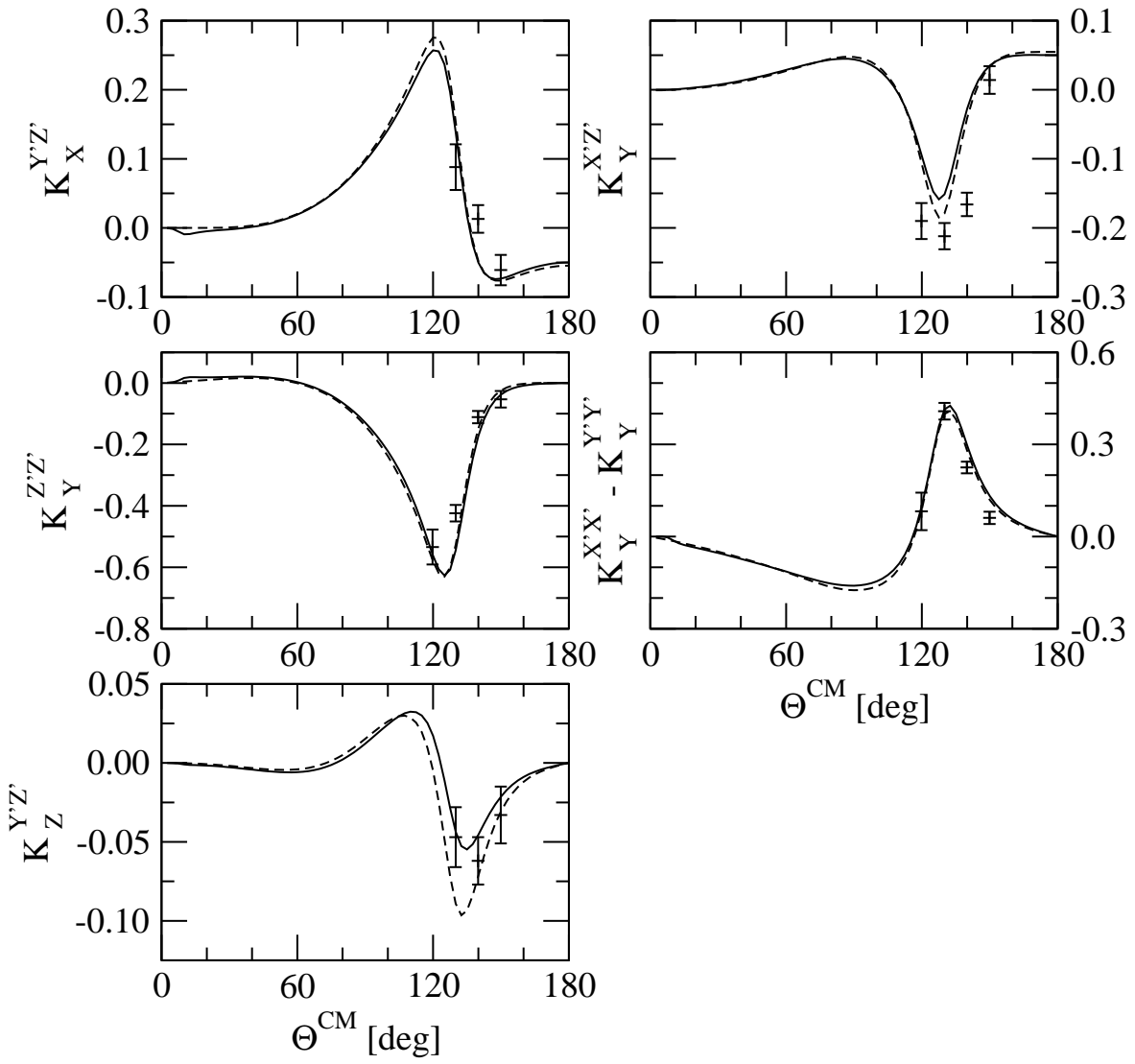


FIG. 3. The nucleon to deuteron spin transfer coefficients in Nd elastic scattering at  $E_{lab}^N = 22.7$  MeV. The description of symbols and lines is the same as in Fig.1.

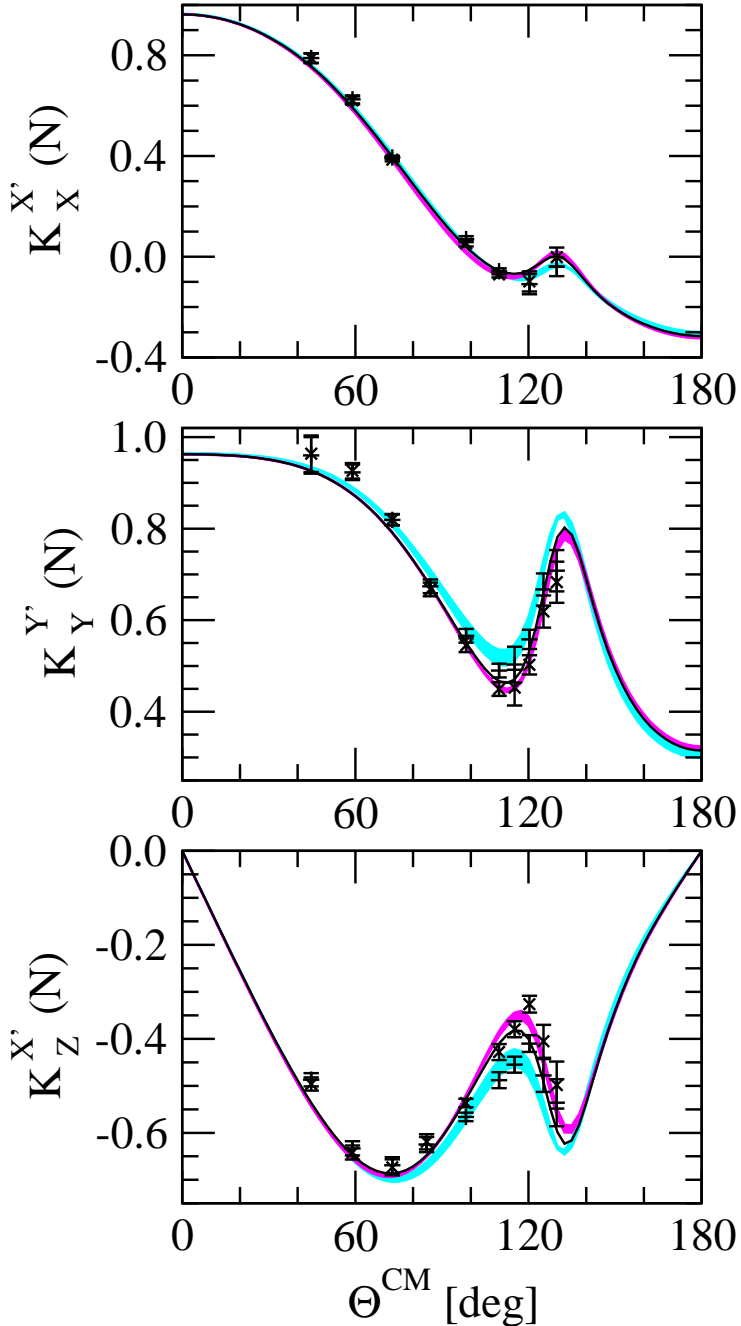


FIG. 4. The nucleon to nucleon spin transfer coefficients in Nd elastic scattering at  $E_{lab}^N = 22.7$  MeV. The crosses are the pd data from [27–29] and x-es are the corresponding “nd data” obtained by subtracting the effects due to the pp Coulomb force (see text for explanation). The light band results from theoretical predictions obtained with the AV18, CD Bonn, Nijm I and II NN potentials. The dark band is obtained when these interactions are combined with the TM99 3NF. The solid line is the prediction of the AV18 + Urbana IX 3NF.

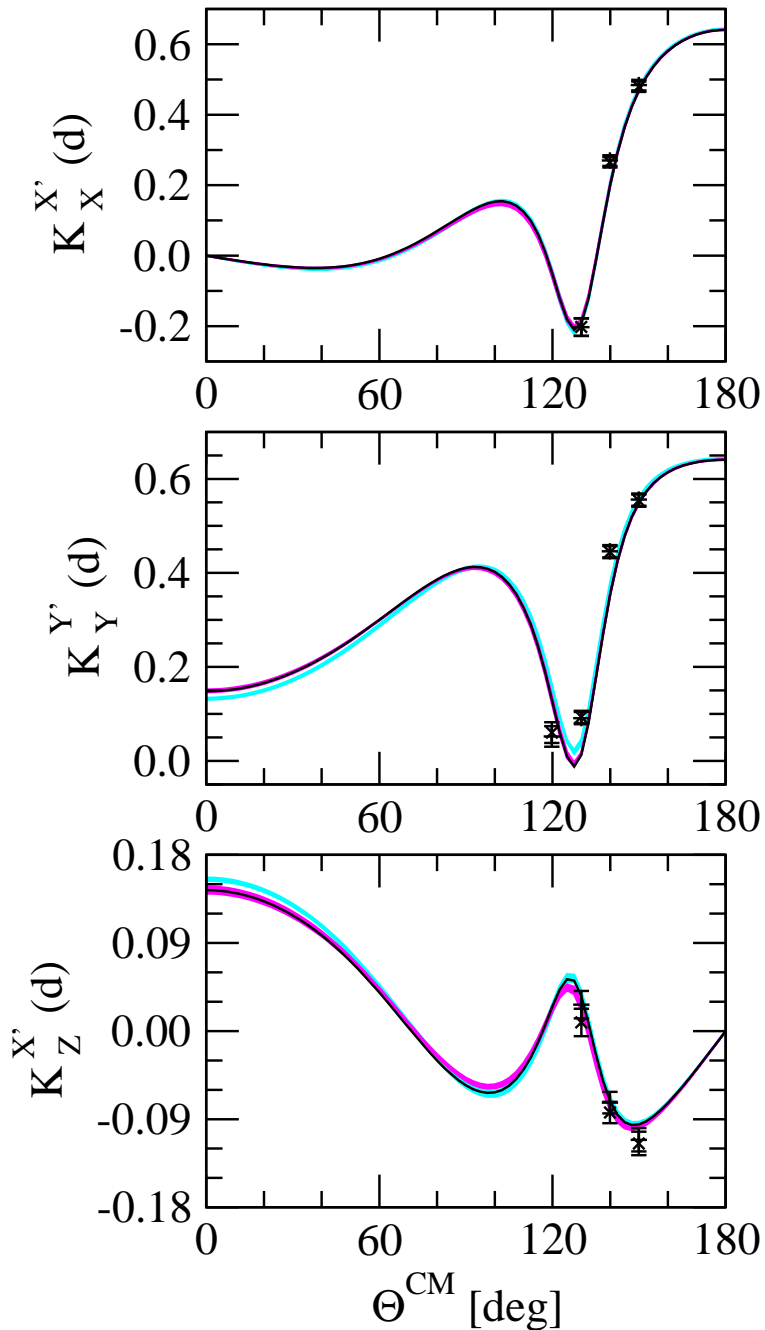


FIG. 5. The nucleon to deuteron spin transfer coefficients in Nd elastic scattering at  $E_{lab}^N = 22.7$  MeV. The description of symbols, bands and lines is the same as in Fig.4.

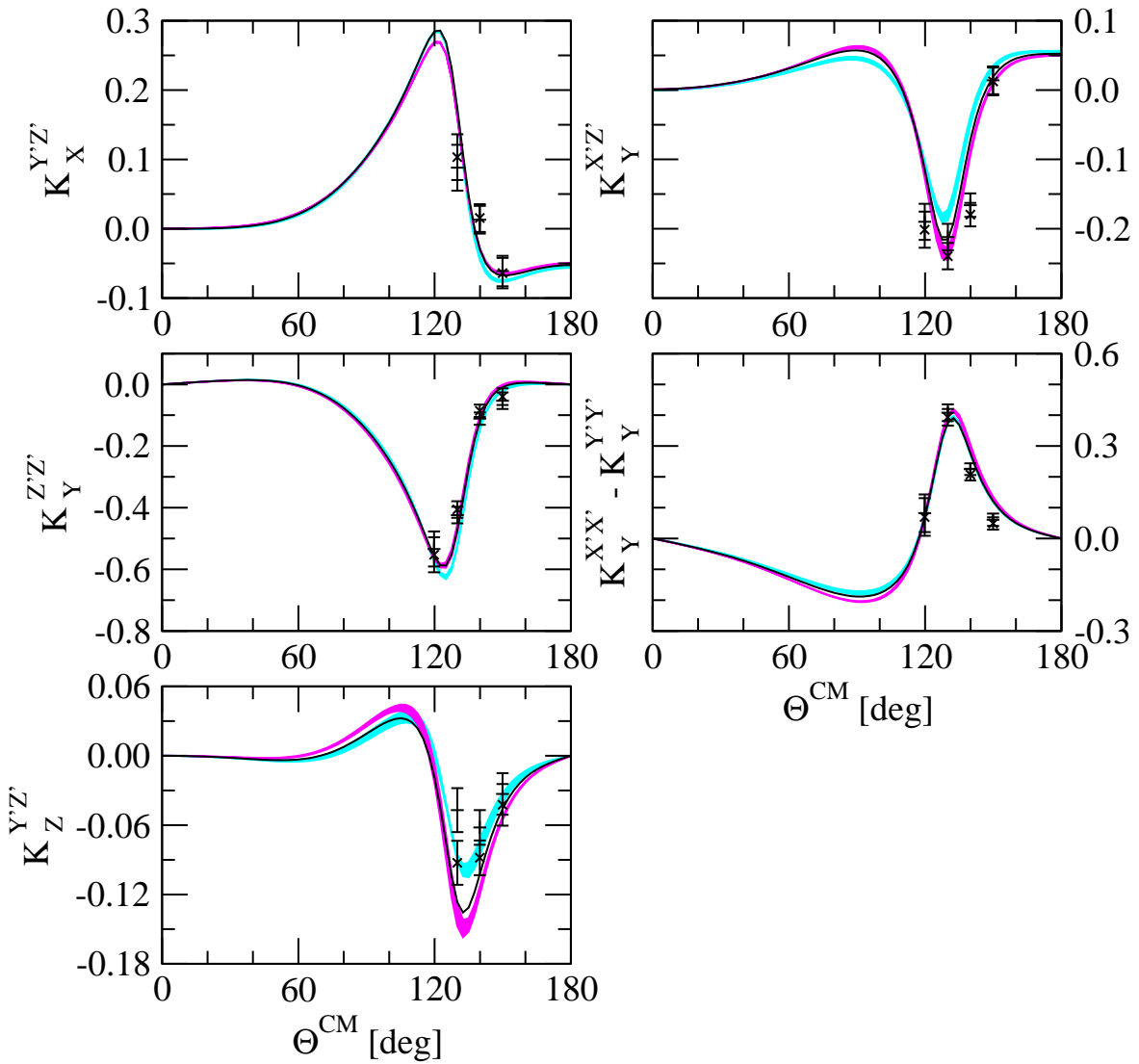


FIG. 6. The nucleon to deuteron spin transfer coefficients in Nd elastic scattering at  $E_{lab}^N = 22.7$  MeV. The description of symbols, bands and lines is the same as in Fig.4.

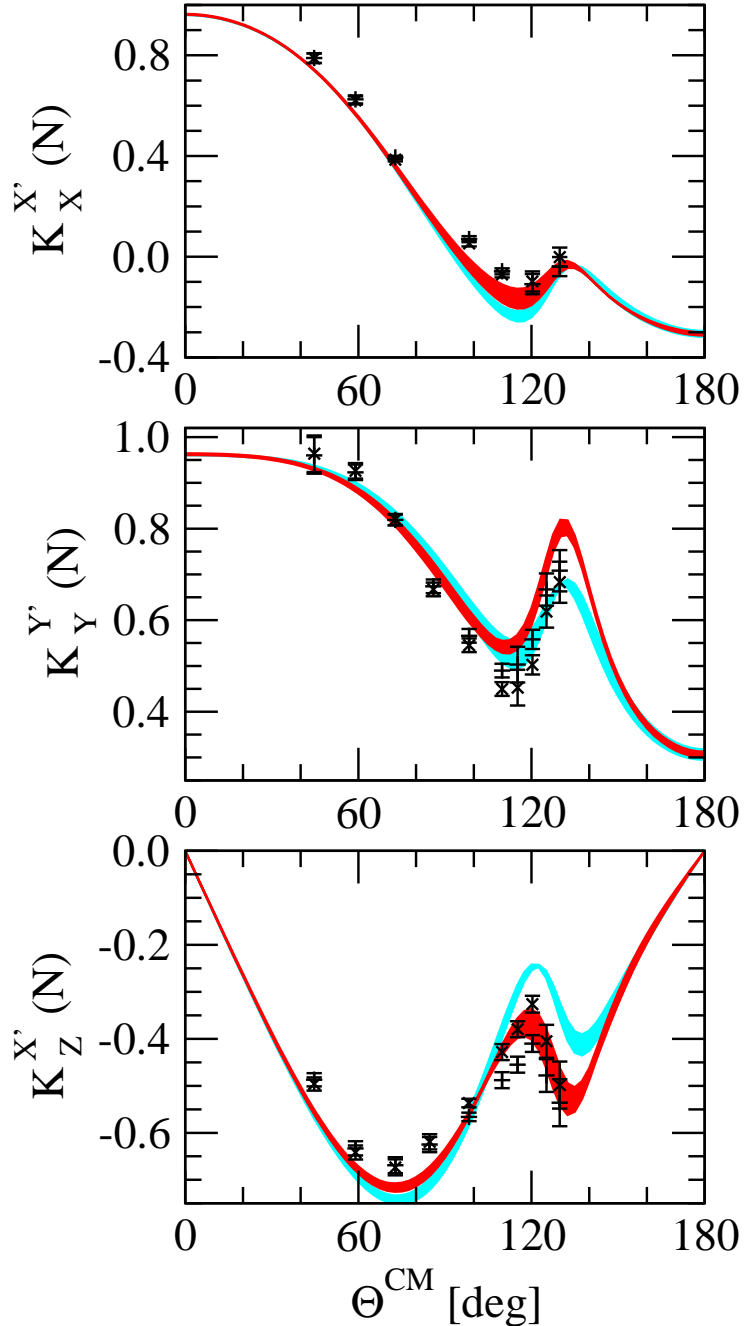


FIG. 7. The nucleon to nucleon spin transfer coefficients in Nd elastic scattering at  $E_{lab}^N = 22.7$  MeV. The description of symbols is the same as in Fig.4. The light band results from theoretical predictions obtained with the NLO chiral potential with different cut-off parameters. The dark band results when in NNLO the NN- and 3N-forces are included.

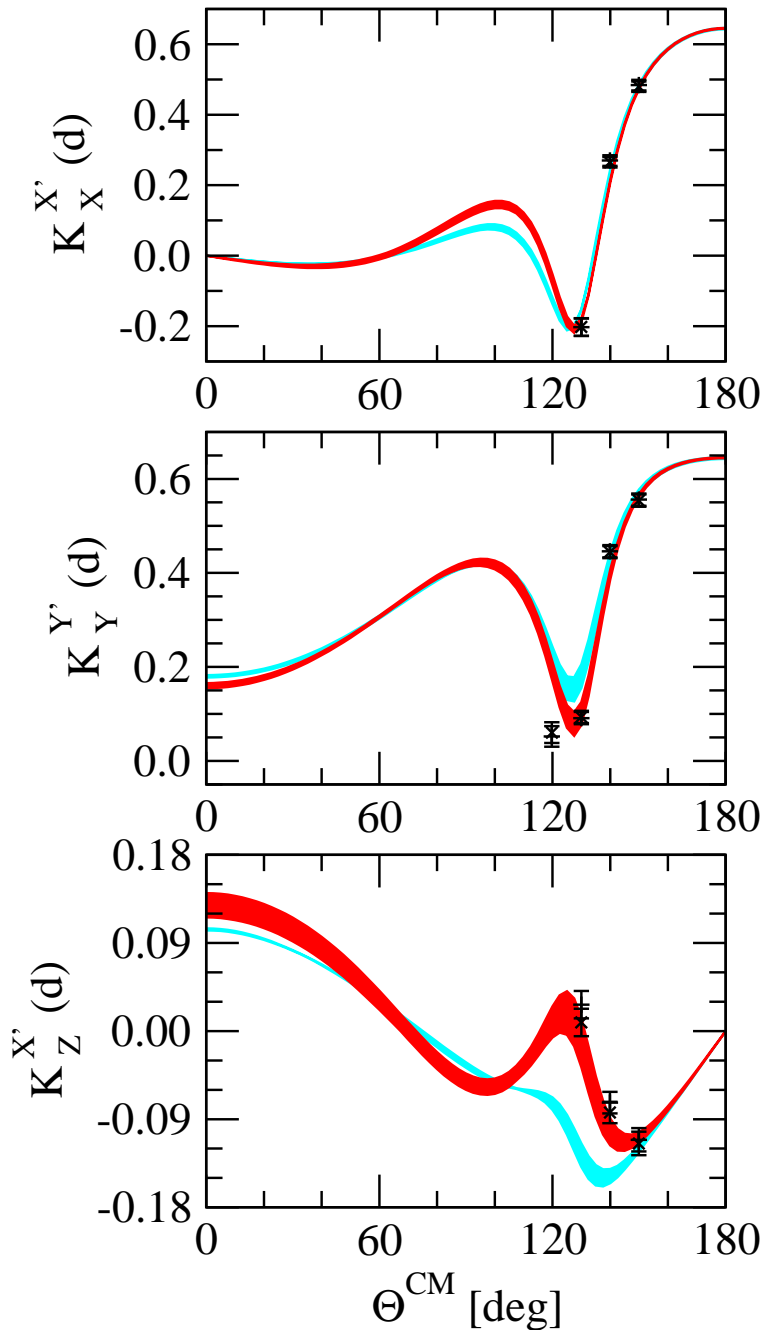


FIG. 8. The nucleon to deuteron spin transfer coefficients in Nd elastic scattering at  $E_{lab}^N = 22.7$  MeV. The description of symbols and bands is the same as in Fig.7.

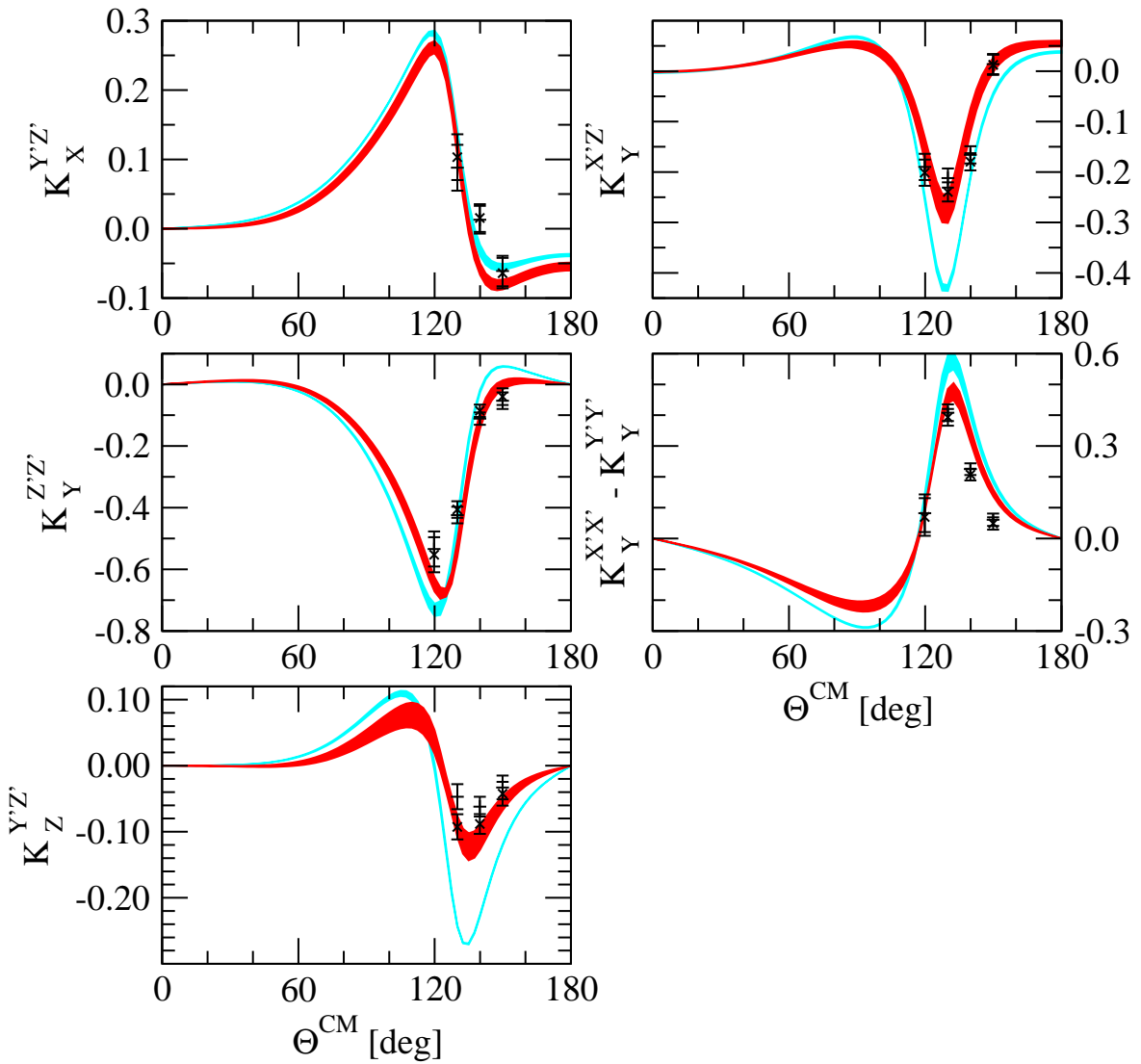


FIG. 9. The nucleon to deuteron spin transfer coefficients in Nd elastic scattering at  $E_{lab}^N = 22.7$  MeV. The description of symbols and bands is the same as in Fig.7.